Indonesian Journal of Aerospace Vol. 23 No. 2 December 2025 : pp 127–146 (Pandie et al.)
DOI: 10.55981/ijoa.2025.13660
https://ejournal.brin.go.id/ijoa/

Structural strength analysis of unmanned aerial vehicle (UAV) wings with varying wingtip extension configurations

Andry Renaldy Pandie[1], Taufik Azhary [2], Aleksey V. Kirillov [3]

[1]PhD graduated from the Department of Aeronautics and Astronautics, Graduate School of Systems Design, Tokyo Metropolitan University, 6-6 Asahigaoka, Hino, Tokyo, 191-0065, Japan
[2]Lecturer at the Department of Mechanical Engineering, Faculty of Science and Technology, Universitas Nahdlatul Ulama Sunan Giri, Bojonegoro, East Java, 62115, Indonesia.
[3]Associate Professor in Aircraft Maintenance and a Senior Researcher in Space Engineering, Samara National Research University, 34, Moskovskoye shosse, Samara, 443086, Russia.
e-mail: andrey.renaldy@gmail.com

Received: 07-11-2025 Accepted: 09-01-2026 Published: 12-02-2026

Abstract

This study investigates the structural performance of three wingtip configurations—single winglet, double winglet, and fence wingtip extension—for UAVs under specified static loading conditions using Patran/Nastran simulations. The analysis focuses on stress distribution and safety margins. The single winglet exhibits maximum stress, highlighting its capacity to safely withstand the applied loads while offering a simple design for easier manufacturing. The double winglet demonstrates reduced maximum stress, reflecting a balanced trade-off between strength and design complexity. The fence wingtip extension achieves the highest structural robustness, showcasing superior load-bearing capacity but with increased manufacturing complexity. The findings reveal that the fence wingtip extension is the most reliable in terms of structural strength and safety, making it suitable for high-performance UAV applications. Meanwhile, the single winglet emerges as the most practical option for cost-efficient production without compromising structural integrity. The double winglet is a viable compromise, combining moderate structural advantages with reasonable manufacturability.

Keywords: Wingtip configurations, Structural strength, Margin of safety, Patran/Nastran simulation.

1. Introduction

The invention of aircraft marks an extraordinary technological advancement for the world. Since humans discovered the ability to fly, aerospace technology has developed rapidly. Innovation in aircraft design continues to progress, with aircraft shape and size evolving. Nowadays, aircraft come in various types, including fixed-wing airplanes, rotary-wing helicopters, air balloons, gliders, and unmanned aerial vehicles (UAVs).

In recent years, the development and utilization of UAVs have increased significantly across various sectors. UAVs are unmanned aircraft controlled remotely via remote control or autonomously through a system pre-configured at a ground control station (Li et al., 2024). Due to their advantages, UAVs are continuously being developed for various purposes, such as aero modeling, territorial mapping, natural disaster monitoring (such as floods and forest fires), industrial and commercial applications (Rovira et al., 2022)(Mohsan et al., 2023), and military defense, where they are employed for bombing and reconnaissance missions.

UAVs comprise various components and structures that operate as an integrated system with inherently limited structural strength. is therefore required to ensure that materials can withstand applied loads and stresses over a specified service life (Pandie et al., 2022). During flight, aircraft experience repeated loading, and continuous exposure to such loads may lead to material fatigue and structural degradation (Pandie et al., 2022). Consequently, structural analysis plays a critical role in UAV design, requiring careful consideration of load

conditions, material properties, and structural configuration. A widely used approach for evaluating structural strength and stress distribution is the finite element method (FEM), which discretizes complex geometries into interconnected elements and solves the governing equations through stiffness matrices and boundary conditions. FEM provides detailed information on displacement, stress, and internal load transfer, enabling accurate assessment of structural performance. In practical engineering applications, commercial finite element software such as MSC Patran/Nastran is commonly employed to implement FEM-based structural analyses, particularly for stress evaluation and safety assessment of aerospace components.

Most UAVs are smaller and lighter than conventional human-crewed aircraft. Due to these size and weight constraints, UAV wings must generate sufficient lift while maintaining adequate structural strength to ensure mission success. The wing is the primary lift-generating component, and its aerodynamic performance is strongly influenced by geometric parameters such as wing planform and wingtip configuration. Common wingtip designs include winglets, tip sails, spiroid tips, C-wings, and fences. In addition to aerodynamic considerations, the structural strength of the wing must be evaluated to ensure safe operation. Structural adequacy is commonly quantified using the margin of safety (MoS), which is derived from the relationship between allowable stress based on material properties and actual stress obtained from numerical analysis.

Modeling and numerical simulation are conducted using Catia for geometric modeling and MSC Patran/Nastran for structural analysis to evaluate stress distribution in wings equipped with different wingtip extensions. In this study, a tapered wing planform with a rectangular configuration is considered, and three wingtip designs—single winglet, double winglet, and fence—are analyzed under identical loading conditions. The objective is to identify the wingtip configuration that provides the most favorable structural performance in terms of stress response and margin of safety for UAV applications.

Accordingly, this study emphasizes a comparative evaluation of wingtip extension structures under controlled conditions, providing structural insights that serve as a preliminary step toward more comprehensive full-wing analyses.

2. Overview of UAV and Engineering Mechanics

2.1. Review about UAV

A UAV is an aircraft that can be remotely controlled by a pilot or fly autonomously using aerodynamic principles (EASA, 2019). In UAV design, mission requirements directly influence wing structural design, particularly in terms of load-carrying capability and stiffness. Wings must generate sufficient lift while maintaining adequate structural strength under operational conditions.

For effective surveillance, UAVs should have a minimum flight altitude of 200 meters, a flight speed up to 100 m/s, and a flight duration of at least 30-60 minutes (Geoscan, 2024) (Seidaliyeva et al., 2024).

To facilitate easy mobilization and demobilization, UAVs must be practical, portable, and capable of hand-launched (Geoscan, 2024). Therefore, the UAV's weight should be under 6 kg. The UAV's airframe must also accommodate various instruments, necessitating a significant lift.

To achieve sufficient lift, the following factors should be considered:

- Adequate wing area (Rohini et al., 2022).
- Use of asymmetrical wing airfoil.

- Wing placement above the airframe.
- Use of a relatively low-powered engine.

Consequently, wing geometry and wingtip configuration play an important role not only in aerodynamic performance but also in determining stress distribution and structural safety. In this study, the structural response of different wingtip extensions is evaluated to assess their influence on stress levels and margin of safety.

2.2. Engineering mechanics

Engineering mechanics is a branch of science that focuses on analyzing forces and moments acting on structures or mechanical systems. In the context of aircraft wing structures, engineering mechanics ensure that structural elements can withstand loads experienced during flight. This analysis is crucial for maintaining the safety and reliability of the aircraft during operation.

The first step in structural strength analysis is identifying the applied loads acting on the wing, including aerodynamic loads and structural self-weight. The wing structure is typically modeled using a cantilever beam approach, where one end of the wing is fixed to the fuselage while the other end is free. This model facilitates the application of beam theory to calculate forces and deformations. Stress and strain quantities are evaluated to assess structural response under applied loads.

For complex structures like aircraft wings, numerical methods such as the Finite Element Method (FEM) are often used to analyze stress and deformation distributions more accurately. Through this approach, wing designs can be optimized to reduce weight without compromising strength and safety.

2.2.1. Support

In engineering mechanics, supports ensure the stability of structures by providing reactions to the loads acting on them. The three main types of supports commonly used in construction, as shown in (Figure 2-1).

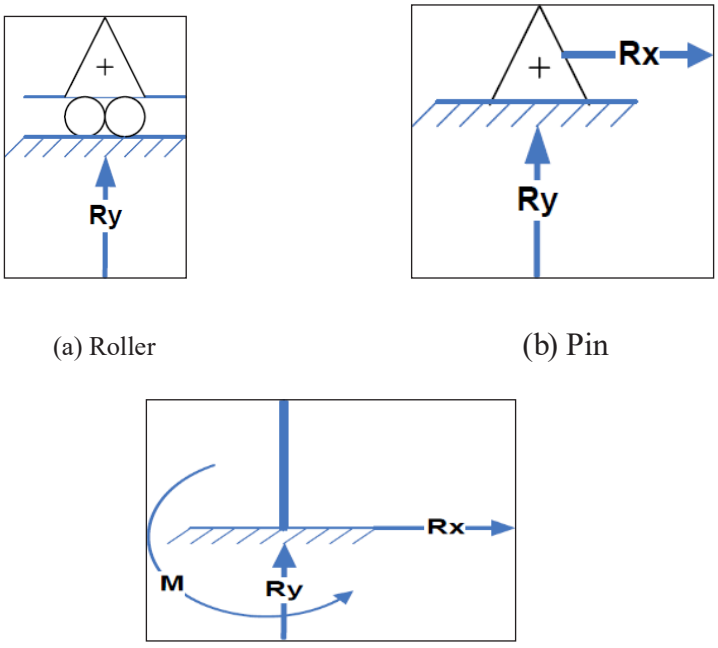

(a) Roller (b) Pin

(c) Fixed

Figure 2-1: Types of support (Irawan, 2007).

In this study, the wing–fuselage connection is modeled as a fixed boundary condition, constraining translational and rotational degrees of freedom at the wing root. This assumption serves as the primary load-transfer mechanism and is commonly adopted in preliminary wing structural analysis.

2.2.2. Load

A load is an action or force exerted on a structure. In engineering mechanics, loads can be classified based on how they act on the structure. In this current study, aerodynamic loads acting on the wing induce bending and shear stresses that are transmitted to the wingtip extensions. In the numerical simulations, identical loading conditions are applied to each configuration to enable a direct structural comparison.

2.2.3. Stress and strain

Stress is a fundamental concept in engineering mechanics that measures the intensity of internal forces acting on a material due to external loads. Stress helps engineers assess the ability of a material to withstand specific forces before it deforms or fails.

$$\sigma = \frac{F}{A} \tag{2-1}$$

Stress can be classified into three primary types based on the direction of the applied force relative to the cross-section: normal stress, shear stress, and torsional stress (Callister, 2007).

Strain (ε), in contrast, is a measure of the deformation or shape change a material undergoes due to applied forces. Defined as the ratio of a material's change in length (Δl) to its original length (l0). Strain helps engineers evaluate how much a material can bend, stretch, or compress before failing. For structures like drone wingtips, strain analysis is often used to predict material behavior under aerodynamic forces and to ensure that deformations remain within the elastic limit.

$$\varepsilon = \frac{\Delta l}{l_0} \tag{2-2}$$

In this study, stress and strain evaluation are used to identify critical regions in wingtip structures and to ensure that deformation remains within elastic limits under the applied loading conditions.

2.2.4. Structural strength

Aircraft structures must be designed with sufficient structural strength to withstand limit and ultimate loads without failure safely or reaching the yield point of the material. In general, the strength of a structure is often associated with the ultimate load of its constituent material. However, there is no definitive limit in this regard. Regarding the mechanical properties of a material under ultimate load, the yield load can be considered the maximum load a structure can withstand before reaching a critical condition, which depends on the material type.

One of the most satisfactory methods for accurately determining structural strength under varied loading conditions is the loading ratio method (R). This method represents the loading condition of a structure in a non-dimensional form as the ratio between the load applied (Papp) to the structure and the allowable load (Pall). Mathematically, this is expressed as:

$$R = \frac{P_{app}}{P_{all}} \tag{2-3}$$

Subsequently, the loading ratio concept is the basis for calculating the margin of safety (MoS) in structural static strength. In this context, the MoS is defined as a measure of the additional capacity or ability available in a structure to safely withstand static loads under the condition where such loads are applied. The general form of the MoS equation is:

$$MoS = \frac{1}{R} - 1 = \frac{P_{all}}{P_{app}} - 1 = \frac{\sigma_{all}}{\sigma_{app}} - 1 \quad (2\text{-}4)$$

where $\sigma_{app} \triangleq \sigma_{max}$ as implemented in Patran/Nastran software. A positive MoS indicates that the structure operates within safe limits, while its magnitude reflects the additional load-carrying capacity of the structure.

3. Gaps of Related Studies and Research Objectives of the Research

3.1. Gaps of related studies

Recent studies have explored structural analysis and optimization of UAV wings. Researchers have investigated the effects of varying wing configurations, including adjustable wingspan (Philips et al., 2024) and different rib and spar arrangements (Son & Afandi, 2018; Uzun et al., 2024). These studies employed finite element analysis to evaluate structural performance, with some incorporating fatigue analysis (Uzun et al., 2024). The importance of aeroelastic behavior in active wing designs has also been highlighted, demonstrating how wing extension affects tip displacement and sweep (Philips et al., 2024). Material selection has also been examined, comparing aluminum and composite structures (Mazhar & Khan, 2010) (Uzun et al., 2024). Overall, these findings indicate that increasing spar numbers generally improve stiffness, while reducing rib numbers may decrease natural frequencies (Son & Afandi, 2018), thereby contributing to the development of lightweight, structurally sound UAV wings capable of meeting diverse flight conditions and safety requirements (Mazhar & Khan, 2010).

In the study by Oktay and Eraslan (2022), the aerodynamic stability of UAVs equipped with morphing wingtips under varying dihedral angles was investigated; however, several limitations highlight opportunities for further research. While the study effectively evaluates stability derivatives, it does not address structural strength or stress distribution, leaving a critical gap in understanding the mechanical implications of morphing wingtips. Additionally, material properties and their influence on structural performance are not considered, nor are aspects related to manufacturability and cost-effectiveness, which are essential for practical UAV implementation.

Similarly, in the study by Setyo et al. (2018), the effect of wingtip fences on UAV aerodynamic performance was evaluated, showing that wingtip fences can reduce vorticity and mitigate tip vortex formation compared to plain wings or wings with rearward fences. However, this work focuses primarily on aerodynamic aspects and does not include a detailed structural analysis of the wingtip configurations. Moreover, only two specific designs—forward and rearward wingtip fences—were examined, leaving other winglet configurations unexplored. Consequently, the structural performance and comparative safety of different wingtip extension designs remain insufficiently addressed in the existing literature.

3.2. Research objective and contribution

The importance of this study stems from the increasing reliance on UAVs across a wide range of applications and research gaps in recent studies, as described in the preceding sections. As UAVs are deployed in increasingly varied and demanding environments, ensuring their structural performance becomes essential for maintaining safety, reliability, and operational

efficiency. Wingtip extensions are widely recognized for their aerodynamic benefits, such as drag reduction, improved lift-to-drag ratios, and enhanced stability. However, these modifications may also introduce additional structural challenges, including increased loads and localized stress concentrations, which must be carefully assessed to ensure structural integrity during operation.

Therefore, based on the background above, this study aims to analyze several essential aspects of wingtip extensions on UAVs by highlighting three main problems. First, the stress distributions occurring in each type of wingtip extension are evaluated. Second, the margin of safety (MoS) for each configuration is calculated to assess the structural capability under the applied loading conditions. Finally, a comparative assessment is conducted to identify the wingtip extension design that offers the highest level of structural safety for UAV applications.

To maintain focus and clarity, a tapered wing planform with a rectangular wing is adopted for the stress analysis. Three wingtip extension configurations are considered: single winglet, double winglet, and fence. The geometric modeling is performed using CATIA V5R16, while the structural simulations are carried out using MSC Patran/Nastran. The analysis focuses on a homebuilt UAV configuration based on the design approach described by Raymer (Raymer, 1992).

Furthermore, the UAV design data has been established, including total weight (WTO), payload weight (WPL), and cruising speed (vcruising), with the airfoil used being NACA 2411. The loads applied to the wingtip extensions during the analysis are point loads placed at the wingtip, and the material used is Al-6061 aluminum. The outcome of this analysis will be the stress experienced by the wingtip extensions, which will be used to assess the safety and structural performance of the designs.

The remainder of this paper is structured as follows. Section 2 briefly mentions about UAV and engineering mechanics, while Section 3 shows the gaps from related studies and the objectives of this paper to tackle the gaps. Section 4 explains the methodology, assumptions, and numerical simulation conditions. Section 5 presents and discusses the result. Finally, Section 6 presents the conclusions, and Section 7 poutlines potential directions for future work.

4. Methodology

In this study, the methodology used to analyze the wing and wingtip extensions of the UAV follows systematic steps that begin with geometric modeling and conclude with structural analysis using the FEM. The process starts with creating a 3D model of the wing and wingtip extensions using CAD software, specifically CATIA. Modeling in CATIA allows designers to accurately represent the wing's geometry, including critical features such as airfoil profiles, tapered planforms, and various wingtip extension configurations.

Once the geometric model is complete, the next step is to prepare the model for analysis. This process involves applying a mesh to the model, where the geometry is divided into smaller elements that are easier to analyze. The proper use of mesh is crucial to ensuring that the analysis results are accurate and representative. Material parameters are also defined at this stage, such as the mechanical properties of Al-6061 aluminum used in constructing the wingtip extensions.

The meshed model is then analyzed using Patran/Nastran software, a tool for conducting finite element analysis. Using Patran, the researcher applies an equivalent static load at the wingtip region to represent a simplified aerodynamic loading condition for comparative

structural assessment. This load application is intended to generate consistent bending effects at the wingtip–wing interface, rather than to reproduce the full spanwise lift distribution experienced during actual flight. This analysis enables the determination of stress values occurring in each wingtip extension design, as well as the calculation of the margin of safety. This approach is expected to gain deep insights into the structural performance of the wing and wingtip extensions and identify the safest and most efficient design for use in UAVs.

To ensure numerical reliability and reproducibility, the finite element model was discretized using an automatic meshing procedure in MSC Patran, employing three-dimensional solid tetrahedral elements. The mesh density was selected to adequately capture geometric features at the wingtip–wing interface while maintaining computational efficiency. Mesh quality was verified to ensure that no elements exhibited excessive distortion, skewness, or negative Jacobian values, which could compromise numerical accuracy.

The following Table 4-1 is the data of the drone specifically designed for use in the analysis conducted in this study.

Table 4-1: UAV's data

Parameter	Unit
Type of UAV	Homebuilt
W_{TO}	3 (kg)
W_{system}	0.948 (kg)
$\upsilon_{cruising}$	11.11 (m/s)
ρ_{200m}	1.20165 (kg/m^3)
υ_{stall}	9.144 (m/s)
Airfoil type	NACA 2411
C_{Lmax}	1.4217
Aspect ratio (AR)	6
λ_W	0.5
Dihedral angle	3°
Flight condition	Cruise

It should be emphasized that the present study is intended as a comparative structural assessment of different wingtips extension configurations rather than a complete structural optimization of the entire wing. To ensure a fair and consistent comparison, all the wingtip configurations were analyzed under identical boundary conditions, material properties, and loading assumptions. The wing–fuselage interface was modeled as a fixed boundary condition by constraining all translational and rotational degrees of freedom at the wing root. This constraint represents an idealized rigid attachment to the fuselage and is commonly adopted in preliminary structural assessments to isolate wingtip structural behavior. Mechanical loads were applied at the wingtip region on the free end of the structure, acting in the direction consistent with the induced bending response.

It is acknowledged that, under real flight conditions, aerodynamic lift is distributed continuously along the wing span and that the maximum structural loads typically occur during critical maneuvers such as dive conditions, defined by the design dive speed (V-ive) and the associated load factor. However, incorporating spanwise-distributed aerodynamic loads and maneuver-based load cases would require a coupled aerodynamic–structural framework and a full-wing structural model, which are beyond the scope of the present study. Therefore,

an equivalent concentrated load is consistently applied across all configurations to enable a direct, objective comparison of stress distributions and margins of safety among different wingtip designs.

Although the interaction between the wingtip and the entire wing structure is acknowledged, modeling the entire wing with distributed aerodynamic loading is beyond the scope of the present work. Such an approach requires a coupled aerodynamic–structural framework and a detailed representation of the spanwise load distribution. Therefore, the current methodology focuses on isolating the structural response of the wingtips to enable a direct comparison between the configurations under controlled conditions.

4.1. Wing and wingtip model

The design of an aircraft wing is a critical component in aircraft development, as it heavily relies on aerodynamic parameters and flight characteristics. In designing one wing, several geometric and aerodynamic parameters are calculated based on formulas provided by Raymer (Raymer, 1992). A detailed explanation of these critical parameters is as follows:

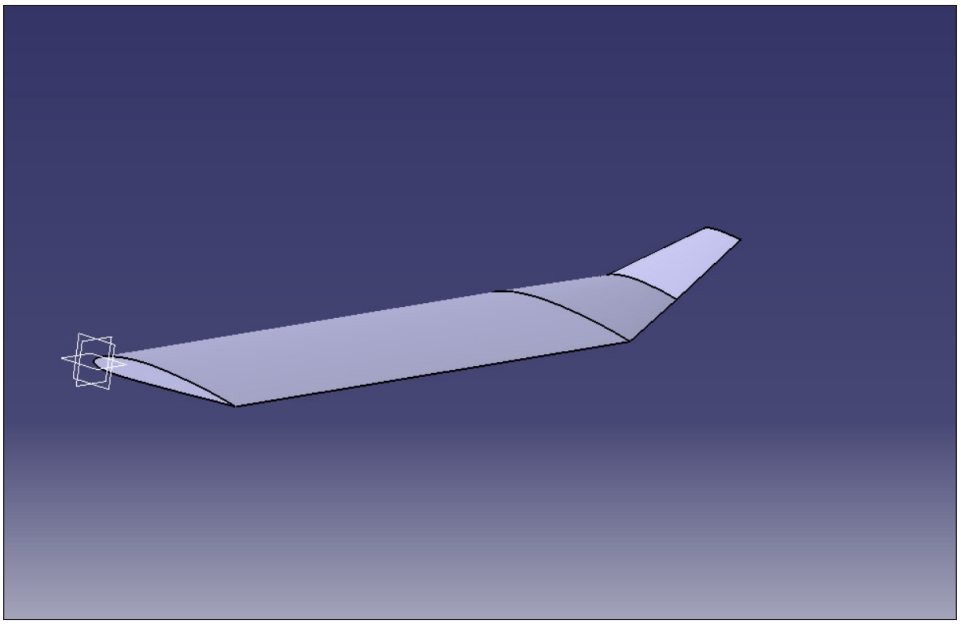

Figure 4-1: Geometry of single winglet.

4.1.1. One wing

The area of one wing is determined by the take-off weight (W_{TO}), air density at a given altitude (ρ_{alt}), stall speed (v_{stall}), and maximum lift coefficient (C_{Lmax}). This relationship is expressed as:

$$S_W = \frac{2W_{TO}}{\rho_{alt} v_{stall}{}^2 C_{L_{max}}} \tag{4-1}$$

This equation 4-1 indicates that a higher stall speed or a lower maximum lift coefficient necessitates a larger wing area to generate sufficient lift.

The wingspan of one wing is calculated using the aspect ratio (AR) and half of the total wing area $\frac{S_W}{2}$, as given by the formula:

$$b = \sqrt{AR\left(\frac{S_W}{2}\right)} \tag{4-2}$$

This parameter is essential for determining the aerodynamic efficiency of the wing.

The root chord, which refers to the chord length at the wing root, is calculated based on the area of one wing (Sw), wingspan (b), and taper ratio ($\lambda_W\lambda_W$) using the following equation:

$$C_r = \frac{S_W}{b(1+\lambda_W)} \tag{4-3}$$

This length determines the size of the wing near the fuselage.

The tip chord, or the chord length at the wingtip, is derived by multiplying the taper ratio ($\lambda_W\lambda_W$) with the root chord (C_r):

$$C_t = \lambda_W\, C_r \tag{4-4}$$

This ratio affects the lift distribution along the span of the wing.

The mean aerodynamic chord represents the average chord length and is computed as:

$$\bar{C} = \frac{2}{3}\left(\frac{1+\lambda_W+{\lambda_W}^2}{1+\lambda_W}\right)C_r \tag{4-5}$$

This parameter is crucial for determining the center of pressure on the wing.

The maximum thickness (Mt) of the wing is defined as 11% of the mean aerodynamic chord ($\bar{C}$):

$$M_t = .11\bar{C} \tag{4-6}$$

This thickness impacts the structural strength and aerodynamic performance of the wing.

Regarding the UAV data presented in Table 4-1 and the equations outlined in Eqs. 4-1 to 4-6, Table 4-2 summarizes the parameters used for designing the wing and wingtip in the CATIA software. Furthermore, the design will undergo additional analysis to evaluate stress distribution and deformation, ensuring that the wing and wingtip can withstand operational loads within the predetermined margin of safety.

Table 4-2: Data on the UAV's wing and winglet

Parameter	Unit
SW	0.042 (m2)
Cr	0.0789 (m)
Ct	0.0395 (m)
$\overline{C}$	0.0614 (m)
MT	6.754E-3 (m)
Single winglet	0.0012 (m2)
Double winglet	0.0024 (m2)

4.1.2. Geometry of single winglet

A winglet is a small, vertical, or angled extension at the tip of an aircraft wing designed to improve aerodynamic efficiency (Govardhan, 2023). Winglets are crucial in reducing drag, and enhancing fuel efficiency and overall performance. Their development is based on principles of aerodynamics, particularly in managing wingtip vortices—circular airflows that form due to pressure differences between a wing's upper and lower surfaces (Utomo, et al., 2024).

As an aircraft flies, high-pressure air beneath the wing tends to flow outward toward the wingtip, while low-pressure air above the wing flows inward. This interaction generates wingtip vortices, which create induced drag. Adding a winglet mitigates these vortices, as the winglet reduces the energy in the spiraling airflow at the wingtip. This reduced induced drag has several operational benefits, including improved fuel efficiency, extended range, and reduced carbon emissions.

(Figure 4-1) illustrates the geometric representation of a single winglet, a common configuration in winglet design for aircraft or UAV wings. A winglet is an additional structure at the wingtips designed to reduce induced drag by managing the airflow around the wingtip. This design balances aerodynamic efficiency with the structural load experienced by the winglet.

In this geometry, the parameters considered are the root chord and tip chord of the winglet. Specifically:

- The root chord of the winglet ($C_{r_{winglet}}$) is set equal to the tip chord of the main wing.
- The tip chord of the winglet ($C_{t_{winglet}}$) is set to 50% of Ct.
- The geometry of endplate or fence wingtip: $\delta = C_{t_{winglet}}$

4.1.3. Creating a wing with wingtip extension in CATIA

Accessing and retrieving data for the NACA 2411 airfoil can be efficiently accomplished through the Airfoil Tools website (http://airfoiltools.com/). The process involves navigating the platform's features, starting with selecting the "NACA 4-digit airfoils", as shown in (Figure 4-2). Users can input "NACA 2411" in the Text search field and initiate the query by clicking the Search button. The system subsequently generates a detailed profile of the NACA 2411 airfoil, including essential information such as geometric and aerodynamic properties. To further access the airfoil's coordinate data, the Send to airfoil plotter option, located adjacent to the profile, facilitates a seamless transition to a coordinate visualization interface. This data is a foundational input for computational modeling or physical design processes in CATIA, ensuring compatibility with various analyses in Patran/Nastran.

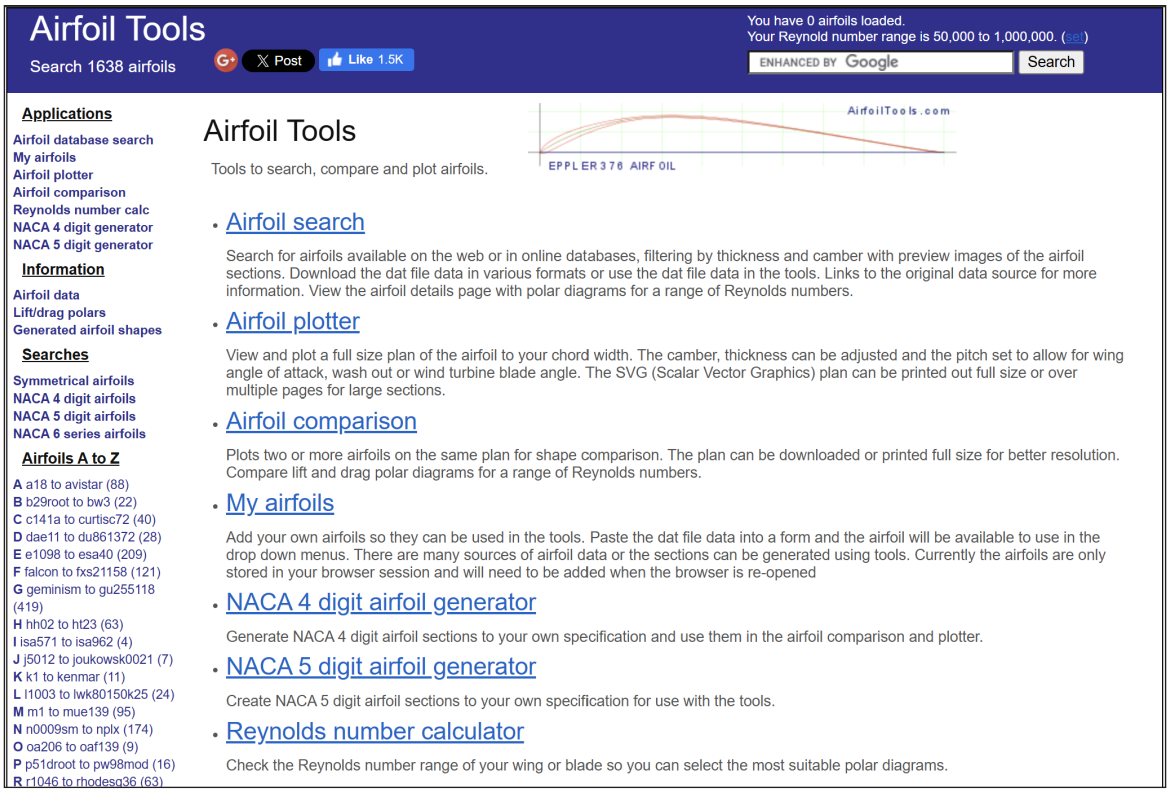

Figure 4-2: Homepage to generate the airfoil. (source: http://airfoiltools.com/)

4.1.4. The reason to use NACA 2411 type

The selection of the NACA 2411 airfoil for designing the UAV's wingtip is based on a combination of aerodynamic and structural considerations, ensuring an efficient and reliable design. As part of the NACA 4-digit series, the NACA 2411 airfoil features a maximum camber located at 20% of the chord from the leading edge and a maximum thickness of 11% of the chord. These characteristics generally make it highly suitable for low-to-moderate speed applications like UAVs, where aerodynamic efficiency and stability are paramount for achieving steady and energy-efficient flight.

In terms of wingtip design, the NACA 2411 airfoil offers advantages in reducing induced drag caused by wingtip vortices. Its low-to-moderate camber facilitates the mitigation of aerodynamic disturbances without compromising lift performance. Furthermore, the selected root chord (Cr = 78.9 mm) and tip chord (Ct = 0.0395 mm) are tailored to achieve an optimal taper ratio based on the calculation as shown in Table 4-2, supporting an even lift distribution along the wing span. This combination enhances aerodynamic efficiency and minimizes structural loads, contributing to overall stability and maneuverability, which were evaluated in this study.

Structurally, the airfoil's selection also accounts for the wingtip's ability to withstand maximum aerodynamic loads during operations, including extreme maneuvers or unpredictable environmental conditions. The chosen chord dimensions help optimize load distribution across the wing, reducing stress concentrations in critical areas and improving structural reliability. Load analysis ensures that the wingtip can endure maximum lift forces with a safety factor typically ranging from 1.5 to 2 times the maximum load. This is further supported by the

appropriate geometric properties and materials, ensuring an adequate margin of safety to accommodate material variations, manufacturing errors, or unexpected overloads.

Subsequently, the application of FEA/FEM is used to examine stress and deformation distributions in the wingtip. By leveraging the NACA 2411 geometry and the selected chord ratio, this analysis provides detailed insights into critical areas prone to structural failure. For instance, the combined bending and shear loads at the wingtip root are a primary focus to ensure the design has sufficient structural capacity. Moreover, the analysis supports weight reduction without compromising safety, improving the UAV's fuel or energy efficiency, and extending its operational duration.

4.1.5. Procedure to design the winglet

The design and analysis of the airfoil used in this study involve several systematic steps to ensure its aerodynamic and structural integrity. The process begins by importing the downloaded airfoil data into CATIA in .csv format, which is downloaded from the Airfoil Tools website.

The next step is to design a double winglet with a 30-degree angle. Winglets are essential to enhance aerodynamic performance by reducing induced drag and improving overall efficiency. Including a double winglet with a specified angle aims to optimize lift distribution while minimizing vortex formation at the wingtips.

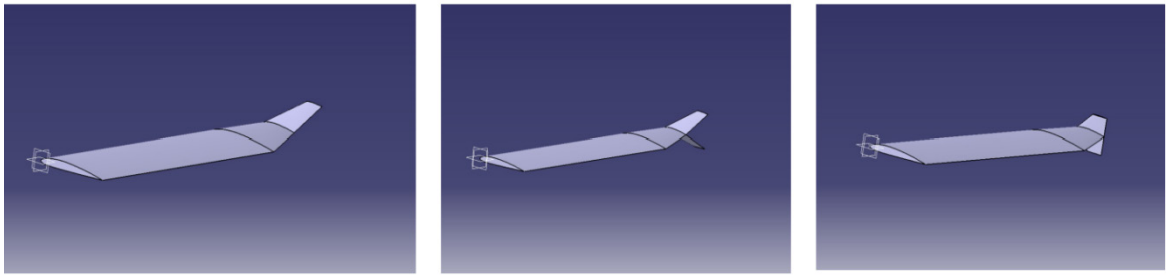

Figure 4-3: Drawings of wing and wingtip extensions (single, double winglet, and fence) modeled in CATIA.

Once the airfoil and winglet design is finalized, the model is exported from CATIA to Patran, a pre-and post-processing software for FEA/FEM. The exported model undergoes a series of preparatory steps for FEA/FEM, starting with defining the material and its properties, as shown in Table 4-3. This involves selecting appropriate materials that provide strength and stiffness while maintaining a lightweight structure. The definition of material is crucial for simulating real-world conditions and predicting the airfoil's behavior under various loads.

Table 4-3: Al-6061 properties (sources:ASTM, 2025 and MatWeb, 2025)

Parameter	Unit
Elastic modulus	6.9E9 (N/m2)
Density	27E2 (kg/m3)
Yield strength	2.78E8 (N/m2)
Poisson ratio	0.33

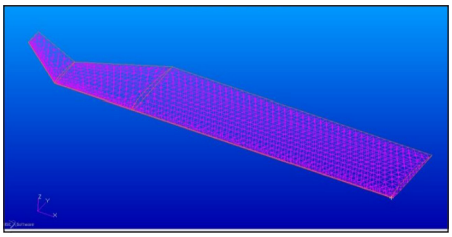

(a) Mesh

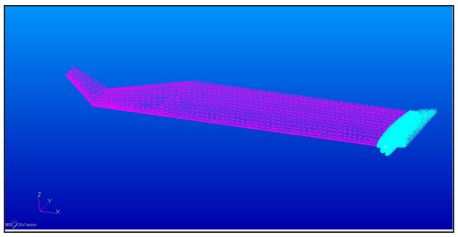

(b) Support

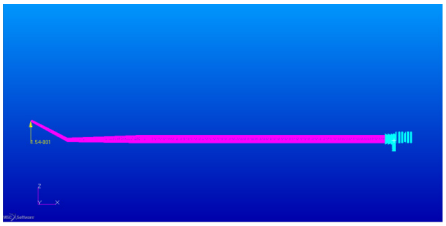

(c) Load (F = 1.5427 N)

Figure 4-4: Wing and wingtip definition in Patran.

4.2. Loading Assumptions and Stress Evaluation Methods

4.2.1. Simulation

Subsequently, for the applied load, the force F acting on the single winglet is 1.5227 N, while for the double winglet, it is 1.5853 N. These force values were derived from the relationship between the lift equation and the wing's mass. They were used as representative static loads to ensure consistency across all wingtip configurations, rather than as exact representations of distributed aerodynamic lift during flight. Additionally, the force applied to the fence wingtip extension is 1.5284 N.

A mesh convergence study was performed to verify the numerical stability of the finite element solution. Several mesh densities with increasing refinement levels were evaluated, and the results were considered converged when the variation in maximum von Mises stress between successive mesh refinements was below 5%. This criterion confirms that the reported stress values are not sensitive to mesh size and provides confidence in the robustness of the numerical results, particularly in the absence of experimental validation. This convergence-based validation approach is adopted as a standard numerical verification method in preliminary structural studies, ensuring that the finite element predictions are governed by physical behavior rather than discretization artifacts.

The finite element model is then subjected to meshing, which discretizes the geometry into smaller elements to facilitate accurate numerical analysis. Following this, constraints and loads are applied to replicate operational scenarios, such as aerodynamic forces, structural loads, and boundary conditions. These specifications allow for a comprehensive assessment of the airfoil's performance and structural integrity.

At last, the analysis is executed using Patran/Nastran, a robust solver that generates results for stress distribution, deformation, and other critical performance parameters. The insights gained from this analysis are vital for identifying potential areas of improvement and ensuring the airfoil design meets performance and safety requirements.

4.2.2. Justification for using aluminum

The selection of aluminum as the primary material for wings in this study offers a unique combination of mechanical properties, cost-efficiency, and manufacturability that remain relevant in UAV design. While composite materials, such as carbon fiber, are often prioritized in high-performance UAVs due to their lightweight nature, aluminum continues to be widely used in specific UAV classes. Its applicability is particularly significant for research involving structural strength analysis, where its properties provide clear advantages:

1. Mechanical reliability: aluminum alloys are known for their consistent and predictable mechanical properties, high strength-to-weight ratio, and excellent corrosion resistance. These characteristics are critical in structural applications, ensuring reliable performance under operational loads. Unlike anisotropic composites, aluminum's isotropic behavior simplifies FEA, enabling accurate and reproducible results.
2. Cost-effectiveness: compared to advanced composites, aluminum is significantly more cost-effective, making it a practical choice for UAVs with constrained budgets, small- to medium-scale prototypes, or research projects. Its affordability ensures that advanced wingtip designs, such as those analyzed in this study, can be implemented without excessive cost burdens.
3. Ease of manufacturing: aluminum is simpler to machine, weld, and form than composite materials. This property is especially advantageous for wingtip designs with intricate geometries, such as the fence wingtip extension, where manufacturing complexity can otherwise hinder production. The manufacturability of aluminum allows for faster iterations and prototyping, making it ideal for academic and industrial applications.
4. Relevance to UAV classes: while composites dominate high-performance UAVs, aluminum remains viable for general-purpose UAVs, tactical drones, and hybrid designs. Its strength, durability, and manufacturing simplicity make it suitable for applications where extreme weight reduction is not the primary focus.

Numerous UAVs, particularly those in military, surveillance, and general-purpose applications, incorporate aluminum or aluminum alloys in their structural components. Notable examples include:

1. MQ-1 Predator by General Atomics (Smithsonian, 2025) : A military UAV that employs aluminum in its fuselage and wings to balance durability and weight, ensuring long-endurance missions.
2. RQ-7 Shadow by Textron Systems (Test, 2025): This tactical reconnaissance UAV uses aluminum in its structural framework, highlighting its suitability for field operations and reliability in diverse environments.
3. Heron by Israel Aerospace Industries (Industries, 2025): Known for surveillance and reconnaissance, Heron utilizes aluminum for structural components, offering resistance to corrosion and operational stability.
4. ScanEagle by Boeing/Insitu (ScanEagle-Insitu, 2025): This compact UAV incorporates aluminum to ensure structural integrity while maintaining a lightweight design for flexible operational scenarios.

The limitation associated with the simplified load application is recognized. Future work will extend the present analysis by incorporating spanwise distributed aerodynamic loads derived from flight envelope conditions, including dive speed and load factor criteria, to enable full-wing structural assessment under critical operational scenarios.

4.2.2. Analytical

To complement the finite element results with a quantitative reference, a simplified analytical stress estimation is introduced as a baseline for comparison. The formulation employed follows the fundamental stress definition previously described in Sections 2 and 4; therefore, only its application to the present wingtip configurations is emphasized here.

Using the representative static loads defined in Section 4 and the effective load-bearing areas summarized in Table 4-2, average stress levels were estimated for each wingtip configuration. The resulting analytical stresses are on the order of 10-5 - 10-4 daN/mm2, ddepending on the wingtip geometry and associated reference area. These values represent global, average stress estimates and are not intended to capture bending-dominated effects or local stress concentrations.

As such, the analytical results serve solely as a lower-bound reference for consistency checking, while the finite element analysis remains the primary tool for evaluating the detailed three-dimensional stress distribution and peak von Mises stress. The comparison between both approaches is presented in the Results section to contextualize the FEM outcomes rather than to establish numerical equivalence.

5. Results and discussion

5.1. Simulation

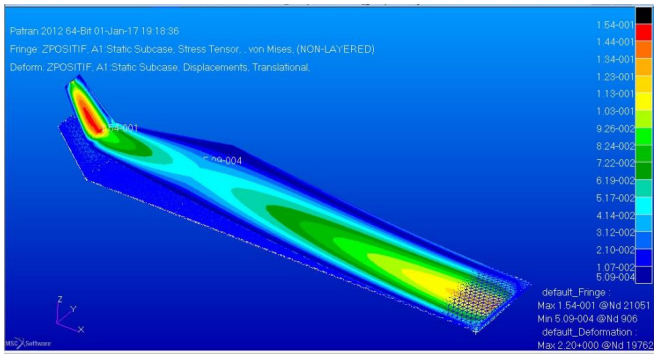

Figure 5-1: Result of force distribution on single winglet.

The structural analysis performed using Patran/Nastran provides insights into the stress distribution on various winglet designs, each evaluated under specified static loading conditions. For the single winglet structure, as shown in (Figure 5-1), the stress distribution is visualized through a color gradient, with red indicating regions of maximum stress and light blue representing areas of minimum stress. The maximum stress value is 1.5401E-1 daN/mm^2 at node 21051, and the minimum stress is 5.09E-4 daN/mm^2 at node 906. This gradient effectively illustrates the load distribution experienced by the winglet during operation. The analysis yielded a *MoS* of 1804.0776, signifying that the structure can safely withstand the

applied loads without the risk of structural failure. These findings validate the reliability and safety of the single winglet design for use in flight scenarios.

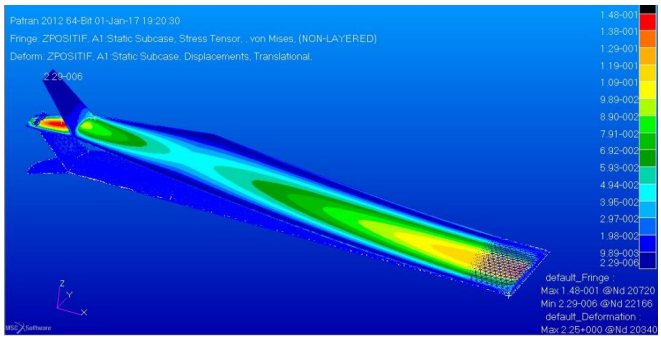

Figure 5-2: Result of force distribution on double winglet.

Extending this evaluation to the double winglet, depicted in (Figure 5-2), a similar analysis was performed to assess its structural performance. The maximum stress was 1.48E-1 daN/mm^2 at node 20720, whereas the minimum stress was 2.29E-6 daN/mm^2 at node 22166. These stress values highlight the load distribution across the double winglet, particularly in critical regions subjected to higher stress. The computed *MoS* for the double winglet is 1877.3784, indicating a robust safety margin far exceeding the maximum applied load. Consequently, the double winglet is also deemed safe and reliable for operation under defined flight loading conditions, demonstrating improved load distribution capabilities.

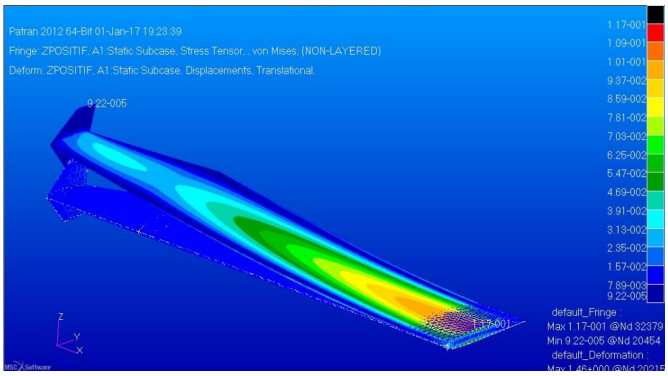

Figure 5-3: Result of force distribution on fence wingtip extension.

Lastly, the fence wingtip extension analysis, visualized in (Figure 5-3), further emphasizes the robustness of these structural components. The stress distribution reveals a maximum value of 1.17E-1 daN/mm^2 at node 32379, while the minimum stress is 9.22E-5 daN/mm^2 at node 20454. This distribution, represented by a color gradient, indicates that higher stress levels are confined to localized regions, while most of the structure experiences significantly lower stress levels. The *MoS* for the fence wingtip extension is calculated as 2375.0684, reflecting a substantial safety reserve and confirming its ability to operate well within structural limits under the specified conditions. These results reinforce the design's reliability and robustness, aligning with the stringent performance criteria required for aerospace applications.

Through this comparative analysis, each design—single winglet, double winglet, and fence wingtip extension—demonstrates high safety margins and reliable performance under the given operational conditions. This highlights their suitability for practical aerospace applications while offering insights into their respective stress behaviors and load-bearing capacities.

Table 5-1: Structural analysis of wingtip extensions.

Extension type	σmax (daN/mm2)	σmin (daN/mm2)	MoS
Single winglet	1.5401E-1	5.09E-4	1804.077
Double winglet	1.48E-1	2.29E-6	877.3784
Fence	1.17E-1	9.22E-5	2375.0684

Based on the structural analysis of the three winglet types—single winglet, double winglet, and fence wingtip extension—as shown in (Figure 5-4), the fence wingtip extension exhibits the highest structural safety margin, indicating its superior ability to withstand applied loads without failure. However, the single winglet achieves a slightly higher maximum stress tolerance than the double winglet and fence wingtip extension. In terms of manufacturability, the single winglet offers a simpler design with fewer components and less complexity, making it easier and more cost-effective to produce. Therefore, while the fence wingtip extension demonstrates the best overall structural strength, the single winglet balances adequate strength and ease of manufacturing. It is a practical choice for applications prioritizing cost efficiency and simpler production.

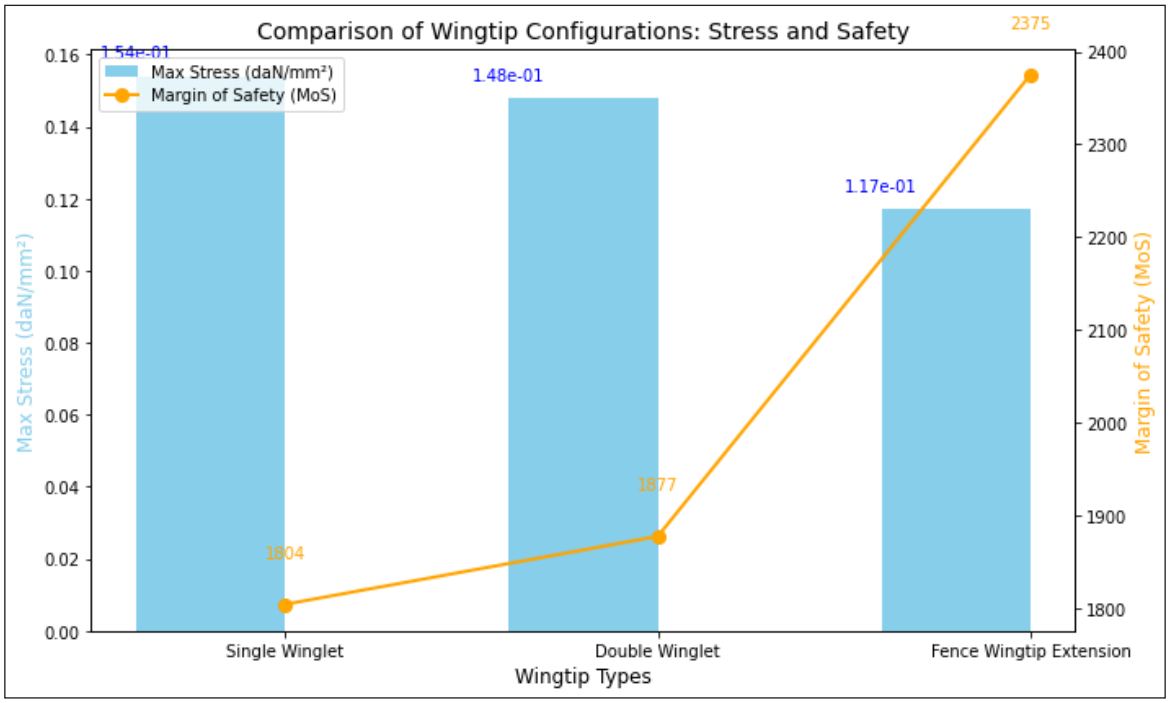

Figure 5-4: Stress and *MoS* of wingtip configurations.

5.2. Analytical

Based on the geometric parameters summarized in Table 4-2 and the applied loads defined in Section 4, analytical stress estimates were obtained for each wingtip configuration. The single winglet exhibits an estimated average stress of 1.27 × 10^{-4} daN/mm² under an applied force of 1.5227 N. For the double winglet, an applied force of 1.5853 N acting over a larger effective area results in a lower estimated stress of 6.61 × 10-5 daN/mm². The fence wingtip extension, evaluated under a force of 1.5284 N using an equivalent effective area assumption, yields an analytical stress of 1.27 × 10-4 daN/mm².

These analytical values represent global average stress levels and do not account for bending effects, geometric discontinuities, or localized stress concentrations. Accordingly, they are expected to be lower than the maximum von Mises stresses obtained from the finite element analysis, which captures the three-dimensional structural response of the wingtip configurations.

5.3. Simulation (FEM) and Analytical Comparison

Table 5-2: Quantitative comparison between FEM and analytical stress estimation.

Wingtip configuration	FEM maximum stress (daN/mm2)	Analytical stress (daN/mm2)	Interpretation
Single winglet	~10-1	~10-4	
Double winglet	~10-1	~10-5	FEM captures bending
Fence	~10-1	~10-4	effects

In addition to the finite element results, analytical stress estimations were calculated to provide a quantitative baseline for comparison. The analytical stresses, derived from average force-to-area relationships, are consistently lower than the FEM-predicted maximum stresses by several orders of magnitude. This difference is expected, as the analytical approach provides a lower-bound estimate that excludes bending moments, geometric complexity, and localized stress concentrations.

In contrast, the finite element model captures the full three-dimensional structural response of the wingtip extensions, including bending-dominated behavior, which governs the peak stress levels. Despite the numerical differences, both analytical and FEM results indicate that the induced stresses remain well below the yield strength of Al-6061, resulting in large margins of safety across all configurations.

Therefore, the analytical calculations serve as a complementary consistency check, while the FEM results provide the primary basis for comparative structural assessment among the wingtip designs.

6. Conclusions

The structural analysis of the single winglet, double winglet, and fence wingtip extension demonstrates varying performance in stress distribution, safety margins, and manufacturing considerations. The single winglet achieves maximum stress, signifying its ability to withstand the applied load safely while maintaining a simpler geometry that simplifies the manufacturing process. The double winglet slightly improves safety capacity while distributing stress efficiently in critical regions. The fence wingtip extension surpasses both configurations with the highest MoS, indicating an exceptional reserve capacity for load-bearing under specified conditions. However, its design may require more complex manufacturing processes.

The fence wingtip extension is the most structurally robust option, providing the highest safety margin and superior reliability for aerospace applications requiring maximum performance. However, for scenarios prioritizing cost-efficiency and manufacturability, the single winglet is a practical choice due to its simpler design and adequate safety capacity. The double winglet offers a middle ground, balancing improved structural strength with moderate complexity. Therefore, the optimal winglet design depends on specific operational and production requirements, with the fence wingtip extension recommended for applications prioritizing strength and safety and the single winglet preferred for streamlined manufacturing and reduced costs.

Future work

To complement this research, potential future work could focus on several areas. First, experimental validation of the simulated stress distributions and MoS using wind tunnel tests or in-flight measurements would provide a more comprehensive understanding of the wingtip structures under real-world conditions. Second, exploring the aerodynamic performance of the wingtip design proposed in this study--single winglet, double winglet, and fence wingtip extension designs, including their effects on drag reduction, energy efficiency, and overall flight stability. Third, a detailed cost-benefit analysis of manufacturing processes for each design, incorporating factors like material requirements, production time, and maintenance costs. Fourth, extending the study to include dynamic loading scenarios, such as turbulence and gust loads, would ensure that the designs are robust under a wider range of operational conditions. Lastly, a complete UAV development project could be undertaken, integrating the findings from this research, where this paper primarily focuses on the structural analysis of wingtip extensions added to the UAV wing. This holistic approach would pave the way for a fully operational UAV design optimized for structural integrity and aerodynamic performance.

Contributorship Statement

Andry Renaldy Pandie: Conceptualization, analysis, writing, editing, supervision. Taufik Azhary: Modeling, writing, and editing. Aleksey V. Kirillov: Writing and editing.

References

Li, W., & Wu, B. (2024). Computational fluid dynamics investigation of aerodynamics for agricultural drones. *Computers and Electronics in Agriculture*, 227, 109528. (https://doi.org/10.1016/j.compag.2024.109528)

A.S. Metals. (2025). *6000 series aluminum alloy*. https://asm.matweb.com/search/specificmaterial.asp?bassnum=ma6061t6 (Accessed January 15, 2025)

Callister, W. D. (2007). Materials science and engineering: An introduction. John Wiley & Sons, Inc.

European Union Aviation Safety Agency (EASA). (2019). Cover regulation to implementing regulation (EU) 2019/947 on the rules and procedures for the opera*tion of unmanned aircraft systems*. https://www.easa.europa.eu/en/document-library/easy-access-rules/online-publications/easy-access-rules-unmanned-aircraft-systems?page=4%23%5FToc18667479

Geoscan. (2024). How to choose UAV. https://www.geoscan.ru/en/products/choose-uav (Accessed October 24, 2024)

Govardhan, D., Narasimha Rao, M. V., Srinivasa Rao, P., Kumar, I., & Nalli, N. (2023). Effect of winglet cant angle on the performance of an aircraft wing. Materials Today: Proceedings. https://doi.org/10.1016/j.matpr.2023.06.408

Irawan, A. P. (2007). Diktat kuliah: Mekanika teknik (statika struktur). Tarumanagara University, Jakarta.

Industries, I. A. (2025). Heron TP – MALE Drone. https://www.iai.co.il/p/heron-tp (Accessed January 27, 2025)

Li, W., & Wu, B. (2024). Computational fluid dynamics investigation of aerodynamics for agricultural drones. Computers and Electronics in Agriculture, 227, 109528. https://doi.org/10.1016/j.compag.2024.109528

Mazhar, F., & Khan, A. (2010). Structural design of a UAV wing using finite element method. Proceedings of 51st AIAA/ASME/ASCE/AHS/ASC Structures, Structural Dynamics, and Materials Conference, Orlando, FL. https://doi.org/10.2514/6.2010-3099

MatWeb. (2025). Aluminum 6061. https://www.matweb.com/search/datasheet.aspx?matguid=b8d536e0b9b54bd7b69e4124d8f1d20a&ckck=1 (Accessed January 15, 2025)

Museums, I. W. (2024). A brief history of drones. https://www.iwm.org.uk/history/a-brief-history-of-drones (Accessed October 24, 2024)

Mohsan, S. A. H., Othman, N. Q. H., Li, Y., Alsharif, M. H., & Khan, M. A. (2023). Unmanned aerial vehicles (UAVs): Practical aspects, applications, open challenges, security issues, and future trends. Intelligent Service Robotics, 16, 109–137. https://doi.org/10.1007/s11370-022-00452-4

Oktay, T., & Eraslan, Y. (2022). Stability evaluation of a fixed-wing unmanned aerial vehicle with morphing wingtip. Journal of Aviation, 6 (2), 103–109. https://doi.org/10.30518/jav.1073417

P., S. S., Sutardi, S., Widodo, W., & Mustaghfirin, M. (2018). Aerodynamics analysis of the wingtip fence effect on UAV wing. International Review of Mechanical Engineering (IREME), 12 (10). https://doi.org/10.15866/ireme.v12i10.15517

Pandie, A. R., Yudiana, A. R., & Hermansah, H. (2022). Fatigue and damage tolerance, prediction of crack propagation on plate using Paris equation and Walker equation. Proceedings of the First Multidiscipline International Conference (MIC 2021), October 30, 2021, Jakarta, Indonesia. https://doi.org/10.4108/eai.30-10-2021.2315783

Phillips, F. R., White, T. D., & Hartl, D. J. (2024). Aeroelastic analysis of adaptive small unmanned aerial system wings. Proceedings of the AIAA SciTech 2024 Forum, Orlando, FL. https://doi.org/10.2514/6.2024-1125

Raymer, D. P. (1992). Aircraft design: A conceptual approach (4th ed.). AIAA Inc., Washington, DC.

Rohini, D., AmarKarthik, A., Abinaya, R., Mathan, A., Midhun, S., & Dhushyanth, D. (2022). Buckling analysis of a commercial aircraft wing box and its structural components using NASTRAN Patran. Materials Today: Proceedings, 66, 895–901. https://doi.org/10.1016/j.matpr.2022.04.521

Rovira-Sugranes, A., Razi, A., Afghah, F., & Chakareski, J. (2022). A review of AI-enabled routing protocols for UAV networks: Trends, challenges, and future outlook. Ad Hoc Networks, 130, 102790. https://doi.org/10.1016/j.adhoc.2022.102790

ScanEagle–Insitu. (2025). ScanEagle. https://www.insitu.com/products/scaneagle (Accessed January 27, 2025)

Seidaliyeva, U., Ilipbayeva, L., Taissariyeva, K., Smailov, N., & Matson, E. T. (2024). Advances and challenges in drone detection and classification techniques: A state-of-the-art review. Sensors, 24 (1). https://doi.org/10.3390/s24010125

Son, L., & Afandi, R. (2018). Analisis frekuensi pribadi dan modus getar struktur pesawat tanpa awak type flying wings. METAL: Jurnal Sistem Mekanik dan Termal, 2(2). https://doi.org/10.25077/METAL.2.2.36-42.2018

Smithsonian. (2025). General Atomics MQ-1L Predator A. https://www.si.edu/object/general-atomics-mq-1l-predator%3Anasm_A20040180000 (Accessed January 27, 2025)

Test, D. O. (2025). Evaluation: RQ-7Bv2 Block III SHADOW – Tactical Unmanned Aircraft System. https://www.dote.osd.mil/Portals/97/pub/reports/FY2020/army/2020rq7b-shadow.pdf (Accessed January 27, 2025)

Utomo, M. S. K. T. S., Yohana, E., Mahendra, C., & Utama, I. Y. (2024). Analysis of blended winglet parameters on the aerodynamic characteristics of NXXX aircraft using computational fluid dynamics (CFD). Results in Engineering, 24, 102901. https://doi.org/10.1016/j.rineng.2024.102901

Uzun, M., Çınar, H., Kocamer, A., & Çoban, S. (2024). Structural and fatigue analysis of a UAV wing. Journal of Aviation, 8 (2), 80–87. https://doi.org/10.30518/jav.1433258